

## ORIGINAL ARTICLE

# New approach for hair keratin characterization: Use of the confocal Raman spectroscopy to assess the effect of thermal stress on human hair fibre

Mohammed Essendoubi<sup>1,2</sup>  | Nada Andre<sup>3</sup> | Bérengère Granger<sup>3</sup> | Celine Clave<sup>3</sup> | Michel Manfait<sup>1</sup> | Isabelle Thuillier<sup>3</sup> | Olivier Piot<sup>1</sup> | Jose Ginestar<sup>3</sup>

<sup>1</sup>EA 7506 Biospectroscopie Translationnelle (BioSpectT), Faculty of Pharmacy, University of Reims Champagne-Ardenne, Reims, France

<sup>2</sup>Biophysic Laboratory, Faculty of Medicine and Pharmacy of Tangier, AbdelMalek Essâdi University, Tangier, Morocco

<sup>3</sup>CFEB SISLEY, Paris, France

## Correspondence

Mohammed Essendoubi, EA 7506 Biospectroscopie Translationnelle (BioSpectT), Faculty of Pharmacy, University of Reims Champagne-Ardenne, 51 rue Cognac Jay, Reims, France; Biophysic Laboratory, Faculty of Medicine and Pharmacy, AbdelMalek Essâdi University, Tanger, Morocco.  
Email: [mohammed.essendoubi@univ-reims.fr](mailto:mohammed.essendoubi@univ-reims.fr)

## Abstract

**Objective:** The objective of our research was to investigate the heat-protecting effect of a product ex vivo and in vivo on human hair fibres.

**Methods:** A preparatory study was carried out in order to determine an optimal threshold of thermal stress. For this, the structure of cross-sections of the hair fibre was observed by optical microscopy. Then, Scanning Electron Microscopy (SEM) and Confocal Raman Spectroscopy (CRS) were applied to analyse ex vivo and in vivo morphological and molecular damage in hair structure after heat stress. Finally, in vivo tests were used to collect consumer perception.

**Results:** The preparatory study enabled us to determine an optimal stress threshold of 10 heating cycle for SEM and 5 heating cycle for CRS. Based on spectral hierarchical classification using Ward's clustering algorithm, the ex vivo Raman results show that the spectral signature of the hair treated and heated is very close to the negative control. This shows that the product preserves the keratin structure after thermal stress. These results were also confirmed by an in vivo Raman analysis performed on hair samples from 5 donors. In concordance with Raman results, SEM shows that treated hair presents lesser "bubbles" and "crackling" on the hair surface. Finally, the in vivo studies proved that hair was more protected from heat.

**Conclusion:** The authors concluded that the product shows protective properties with respect to morphological and molecular heat damage. We also demonstrate that the product promotes the  $\alpha$ -helix keratin conformation and preserves the S-S disulfide bands.

This work was the subject of a poster presentation in: The International Society for Biophysics and Imaging of the Skin (ISBS) 2021 digital congress. June 03-05 2021 Berlin, Germany.

The Cosmetic Measurement & Testing (COMET) congress. July 05–06 2022 Cergy, France.

This is an open access article under the terms of the [Creative Commons Attribution-NonCommercial-NoDerivs](https://creativecommons.org/licenses/by-nc-nd/4.0/) License, which permits use and distribution in any medium, provided the original work is properly cited, the use is non-commercial and no modifications or adaptations are made.

© 2022 The Authors. *International Journal of Cosmetic Science* published by John Wiley & Sons Ltd on behalf of Society of Cosmetic Scientists and Societe Francaise de Cosmetologie.

**KEY WORDS**

chemical analysis, Confocal Raman Spectroscopy, hair treatment, scanning electron microscopy, thermal stress, thermo-protective effect

**Résumé**

**Objectif:** L'objectif de notre étude est d'évaluer ex vivo et in vivo l'effet thermo-protecteur d'un produit sur les fibres capillaires humaines.

**Méthodes:** Une étude préparatoire a été réalisée afin de déterminer un seuil optimal du stress thermique. Pour cela, la structure des coupes transversales des cheveux a été observée par microscopie optique. Ensuite, la microscopie électronique à balayage (MEB) et la spectroscopie confocale Raman (SCR) ont été appliquées pour analyser les dommages morphologiques et moléculaires (ex vivo et in vivo) de la structure du cheveu après un stress thermique. Enfin, des tests in vivo ont été réalisés pour recueillir la perception des consommateurs.

**Résultats:** L'étude préparatoire nous a permis de déterminer un seuil de stress thermique optimal correspondant à 10 cycles de chauffage pour la MEB et 5 cycles de chauffage pour la SCR. Basés sur une classification hiérarchique utilisant l'algorithme de Ward, les résultats Raman « ex vivo » montrent que la signature spectrale des cheveux traités et chauffés est très proche du témoin négatif. Cela montre que le produit préserve la structure de la kératine après un stress thermique. Ces résultats ont également été confirmés par une analyse Raman « in vivo » réalisée sur des échantillons de cheveux de 5 donneurs. En concordance avec les résultats Raman, la MEB montre que les cheveux traités présentent moins de « bulles » et de « craquelures » à la surface des cheveux. Enfin, l'étude in vivo a prouvé que les cheveux sont mieux protégés de la chaleur.

**Conclusion:** Les auteurs ont conclu que le produit présente des propriétés protectrices vis-à-vis des dommages thermiques morphologiques et moléculaires. Nous avons démontré également que le produit favorise la conformation de la kératine en hélice- $\alpha$  et préserve les bandes disulfures S-S.

**INTRODUCTION**

The hair, like the skin, undergoes various internal and external aggressions. Among the external aggressions, we have the environmental factors but also the accumulation of numerous chemical or physical treatments [1] that attack and weaken the hair fibre. The use of heat styling appliances such as straighteners, curling irons and hair dryers is becoming more and more common. However, the temperature of these appliances can reach extremely high levels of heat and this heat stress causes long-term damage to unprotected hair, and this damage is cumulative. Moreover, this damage is not limited to the surface of the hair (depletion of the protective lipidic film, cracks in the cuticle and detachment of the scales) [2], it also damages the fibre in depth (evaporation of water and appearance of heat bubbles and degradation of keratin, a heat-sensitive

protein) [3]. The hair then becomes rough, dry, dull and brittle with split ends.

The hair fibre is the visible part of the hair, it is made up of keratinized cells arranged in three layers: the cuticle, the cortex and the marrow. Human hair is mainly constituted of keratin: a hard and fibrous protein substance that gives the hair its strength and elasticity. It is made up of long chains of amino acids, including cysteine, rich in sulfur, which plays an important role in the cohesion of the hair. In fact, the keratin chains are sealed to each other by:

1. Disulfide bridges: stretched between two neighbouring cysteines, these bonds are very strong and are truly characteristic of the keratin structure. However, they are also the weak point of the hair structure because they are sensitive to attack.

2. Weak bonds (salt bridges and hydrogen bonds): The keratin chains are organized into protofibrils, then into microfibrils which are themselves the constituents of the macrofibrils.

Several physical techniques have demonstrated the importance of hair analysis in different fields such as medical, environmental, cosmetic and forensic sciences. Some studies report the use of trichoscopy, x-ray diffraction, solid state nuclear magnetic resonance, circular dichroism, scanning electron microscopy and high-pressure liquid chromatography–mass spectrometry for human hair fibres analysis [4–9]. Although widely accepted, these methods lack accuracy and spatial resolution and they give only surface or structural information without any accurate molecular information. In addition, these techniques present some technical limitations related to protocol complexities, prior sample preparation, the need for extraction and reagent costs. These techniques are therefore not suitable for routine application in cosmetic laboratories [10].

Other spectroscopic techniques are finding their way into the cosmetic field and have been proposed for the investigation of human hair fibres. Both Fourier transform infrared (FTIR) and Raman spectroscopy have been extensively used to probe hair chemical composition and keratin structural changes under different treatments [11–14]. These powerful approaches represent analytical, non-destructive and dynamic methods to investigate changes in whole hair fibre with only little biomass and without any labeling or sample preparation or extraction. The FTIR and Raman spectra constitute very specific spectroscopic fingerprints which reflect the chemical composition and the structure of the hair fibres. This makes it possible to investigate the influence of chemical and physical treatments (active ingredient, reduction, heating, UV exposition and oxidation) on the structure of keratin in human hair fibres [12, 13, 15]. Previous research suggests that FTIR spectroscopy can be proposed, for example, for distinguishing hair follicle tissue layers based on their molecular structure, for discriminating untreated from treated hair, or also for monitoring the chemical changes related to the aging effect of human hair fibre [11, 16]. In parallel, Raman spectroscopy has been used successfully to study L-Phenylalanine and hydrolyzed egg white protein penetration into keratin fibres, to detect the structural change in keratin after chemical treatments or more recently by our team to analyse conformation changes in human hair keratin after active ingredient application [10, 14, 16].

In the present study, the aim is to evaluate a thermoactive hair care product that protects the hair from heat, acting as a heat shield to preserve the fibre of heating devices. The use of hair irons at high temperatures in

addition to hair dryers causes hair damage. The cuticles which make up the surfaces of hair are known to have “lift-ups” and to form “blisters” that are porous flares in hair caused by the heat treatment [2]. For this, we analyse the morphological and molecular changes incurred in the structure of hair samples after thermal treatments with a straightening iron at 235°C. Different methods have been investigated in order to assess the hair damage after the heat stress: (i) for morphological analysis, Scanning Electron Microscopy (SEM) has been used in order to examine the surface of hair fibres. (ii) Raman microspectroscopy to investigate, *ex vivo* and *in vivo*, the molecular thermal damages of keratin in human hair fibres by a direct confocal measurement and (iii) finally an *in vivo* test to collect the consumer perception combined with a hairdresser assessment about the efficiency. By comparing the information provided from those techniques, it will be possible to correlate keratin molecular changes with the morphological information and the structural integrity of the hair fibres as well as the consumer perception of their hair.

## MATERIALS AND METHODS

### Hair care product composition (INCI list)

Aqua/water/eau, butylene glycol, glycerin, brassicamido-propyl dimethylamine, c13-15 alkane, parfum/fragrance, caprylyl methicone, hydroxyethylcellulose, pentylene glycol, stearyl alcohol, camellia oleifera seed oil, moringa oleifera seed oil, hydrolyzed cottonseed protein, polyquaternium-28, dimethicone, citric acid, cetearyl alcohol, polyquaternium-47, disodium edta, cetareth-33, pvm/ma copolymer, dimethiconol, caprylyl glycol, glycine soja (soybean) oil, sodium hydroxide, sorbic acid, phenoxyethanol, sodium benzoate, potassium sorbate, tocopherol, limonene, citral, eugenol, linalool.

### Human hair samples collection and treatment

Standardized hair tresses were provided by Kerling International (KERLING INTERNATIONAL HAARFABRIK GMBH; D-71522 Backnang - Waldrems Postfach 1330). These standardized tresses mean that the hair fibres were obtained from several donors and standardized according to the origin, colour, treatment and length. For the present study, the work was done with standardized stresses of European origin (several donors), 13 cm long and 2 mm large and shade 9/0 (blond) (reference Glued Hair Weft). In order to limit fluorescence

interference during Raman measurements, we used natural light blond hair. The care product was applied at 10% of the tresses weight for 5 min (mean weight of tresses:  $336 \pm 13$  mg; mean quantity of test product applied:  $34 \pm 2$  mg). The tresses received the application of heat directly from the straightening iron at  $235^\circ\text{C}$  over the entire length of the hair shaft. Five or 10 cycles of the heating process were done (one cycle is equivalent to 5 s of heating at  $235^\circ\text{C}$  followed by 15 s of cooling at room temperature). In this work, a flat iron model Babyliiss i-pro 235 ionic XL Wet&Dry was used.

## Preparatory study

A study of a wide range of deterioration with heat was initially studied. Different heating cycles (0, 5 and 10) were applied to hair fibres in order to reveal the conditions allowing visualization of molecular changes without harmful effects on hair fibre morphology.

In the first step, the cross sections of the hair fibres were carried out after applying different heating cycles. In order to evaluate the degree of deterioration of the hair fibre after heat stress and to choose an optimal stress threshold to conduct the study, a comparison of the hair sections was carried out by an optical microscope with a  $100\times$  objective. For this, Optimal Cutting Temperature (OCT) compound was used to embed hair samples prior to frozen sectioning on a cryostat ( $-20^\circ\text{C}$ ). After the heating cycles, the hair samples become brittle and break easily. For this, they must be handled and included gently in the OCT to avoid morphological deformations and curvatures. After rapid freezing at  $-80^\circ\text{C}$ ,  $10\ \mu\text{m}$ -thick transverse sections were cut by cryostat, and three sections per sample were placed onto CaF<sub>2</sub> slides for optical microscope analysis. These observations were also correlated with the images observed with SEM in order to choose the degree of heat stress to be applied in the study. For this purpose, hair fibres after (0, 5, and 10) heating cycles were observed with SEM for evaluation of morphological changes after heat stress.

## Scanning electron microscopy observation

Hair tresses were shampooed (with a classic lauryl sulfate based shampoo) in order to eliminate residues on hair before SEM observations as following procedure:

Tresses were wet with tap water. Excess water was removed with gloved fingers. The shampoo was then deposited onto the hair tresses and 20 rotations over the entire length of the tresses were done until foaming. Finally, hair tresses were rinsed before ambient air drying. Several

hair fibres per case were observed (at least 4 per case). The morphology of hair samples after thermal treatment was examined by a scanning electron microscope (MEB-FEG ZEISS GeminiSEM 300). The samples were placed on specimen mounts using double-sided adhesive tape and were made electrically conductive by coating them with a thin layer (2 nm) of gold (Agar manual Sputter Coater). The pictures were taken at a working distance (WD) between 6.2 and 6.5 mm and EHT (Electron High Tension) between 2 and 8 kV.

## Raman spectroscopic analysis

### Raman spectrometer

Raman spectral acquisitions of hair samples were recorded using a Labram microspectrometer (Horiba Jobin Yvon). The set-up included a microscope (Olympus, BX41) equipped with a computer-controlled motorized  $x$ - $y$  stage, which enabled automatic scanning of the sample with a spatial resolution of  $1\ \mu\text{m}$ . Raman measurements were recorded by using a dispersive Raman spectrograph (Labram, Horiba Jobin Yvon) via a  $100\times$  (0.8 N.A.) long working distance objective (Olympus) operating in air. The objective was mounted on a high-precision piezoelectric device (Physics instrument, Germany) which allowed focusing the laser light on each measuring point of the hair sample. This objective collected light that was scattered by the sample, which was then detected by a charge-coupled device (CCD) detector of  $1024 \times 256$  elements cooled by Peltier effect at  $-65^\circ\text{C}$ . The spectrometer comprises also a grating of 950 grooves/mm permitted to collect data with a spectral resolution of  $4\ \text{cm}^{-1}$ . The confocal hole was set at  $150\ \mu\text{m}$ , assuring an axial resolution of approximately  $2\ \mu\text{m}$ .

The excitation source was provided by titanium-sapphire laser (Model 3900S, Spectra-Physics, France) generating a laser beam with a 785 nm wavelength and operating at 50 mW under the microscope objective, which is non-destructive for hair samples and does not cause any thermal or photochemical degradation. The laser wavelength excitation was chosen as the optimal compromise to ensure the reduction of parasitic fluorescence generation, good penetration of the light deep into the hair samples and sensitivity of the CCD detector over the spectral range.

### Confocal measurements ( $Z$ ) on hair fibres

The axial  $Z$  profiles were recorded directly on a hair fibre for each sample and without any particular preparation.

For the choice of the mapping ( $Z$ ) profile, we visualized the hair fibre with 3 objectives (10 $\times$ , 50 $\times$  and 100 $\times$ ) of the camera microscope (Figure 1).

The mapping ( $Z$ ) profiles consist of an in-depth scanning through the hair fibre. Raman spectra were collected at different focus points, from the surface  $Z = 0 \mu\text{m}$  to  $30 \mu\text{m}$  with a  $3 \mu\text{m}$  step. The spectral acquisitions were recorded on the  $400\text{--}4000 \text{cm}^{-1}$  spectral range at different focus points, taking into consideration the cortex and the cuticle of the fibres in each measurement. Figure 2 shows the spectra corresponding to each depth of the hair fibre up to  $30 \mu\text{m}$  and with a step of  $3 \mu\text{m}$ . The areas under the curve (AUC) of the full spectrum for each depth are displayed in this figure.

For each spectrum, one accumulation of 50 s of laser exposure was taken. Data acquisition was performed using LabSpec 5 software (Horiba Jobin Yvon). Prior to data acquisition, the instrument was calibrated to the  $520.7 \text{cm}^{-1}$  Raman line of silicon and the laser power at the sample level was regularly controlled.

## Data pre-processing and profiles analysis

The spectral data processing methods used in this study were previously described in our work based on the analysis of human hair fibre by Raman spectroscopy [10]. Briefly, in the current study the spectral acquisitions were recorded on the  $400\text{--}4000 \text{cm}^{-1}$  spectral range. Prior to data processing on all Raman spectra, the  $400\text{--}3600 \text{cm}^{-1}$  spectral range was extracted. Beyond  $3600 \text{cm}^{-1}$  Raman spectra do not present any molecular information. The pre-processing of spectral data was performed using LabSpec 5 software (Horiba Jobin Yvon). First, cosmic radiation was removed and all aberrant profiles were excluded from the database. Each remaining profile was subjected to corrections to clean up the Raman signal for the hair fibres. These corrections applied to the raw spectral data

included the correction of spectral shifts, noise reduction using a 5-point average Savitzky–Golay smoothing filter, and baseline correction using a polynomial function of degree 5 to remove the fluorescence background. Finally, for spectral data processing, the set of spectra were vector normalized across the entire spectral range ( $400\text{--}3600 \text{cm}^{-1}$ ). Three axial  $Z$  profiles were recorded for each hair sample, and mean Raman spectra were calculated to ensure that the Raman measurements were reproducible. Due to the irregularity of the flatness of the hair surface, the surface point can slightly vary and no longer corresponds to the zero position ( $Z = 0$ ) of the objective lens shift operated by the piezoelectric device. The surface point is estimated at the half-maximal intensity of CH vibration ( $2800\text{--}3000 \text{cm}^{-1}$ ) when the lower half of the laser beam is in the hair fibre and the upper half is in the air. In this case, the maximum focal point is located exactly at the hair surface. The offset calculated at the surface position was also used to correct the depth of all spectra of the same profile. For further data processing, the average spectra from surface point ( $Z = 0$ ) to  $30 \mu\text{m}$  of depth ( $Z = 30 \mu\text{m}$ ) were calculated for each profile. These average spectra from  $30 \mu\text{m}$  have been used in the analysis, taking into account the molecular information of hair in the cortex and the cuticle.

After the pre-processing steps were completed, the corrected average spectra from  $30 \mu\text{m}$  were processed using self-coded software based on a hierarchical classification algorithm and Amide I band curve-fitting methods operating in the Matlab environment (The Math Works Inc.). The average spectra from axial ( $Z$ ) profiles of hair fibres were classified using Ward's clustering algorithm. This function calculates Euclidean distances between the spectra and groups them into clusters according to their similarities. This method of cluster analysis allows for the classification of hair fibres with a similar keratin structure. The results are shown as a dendrogram. Curve fitting may be used when the resolved features of overlapping Raman bands are difficult to observe. In our analysis, curve-fitting

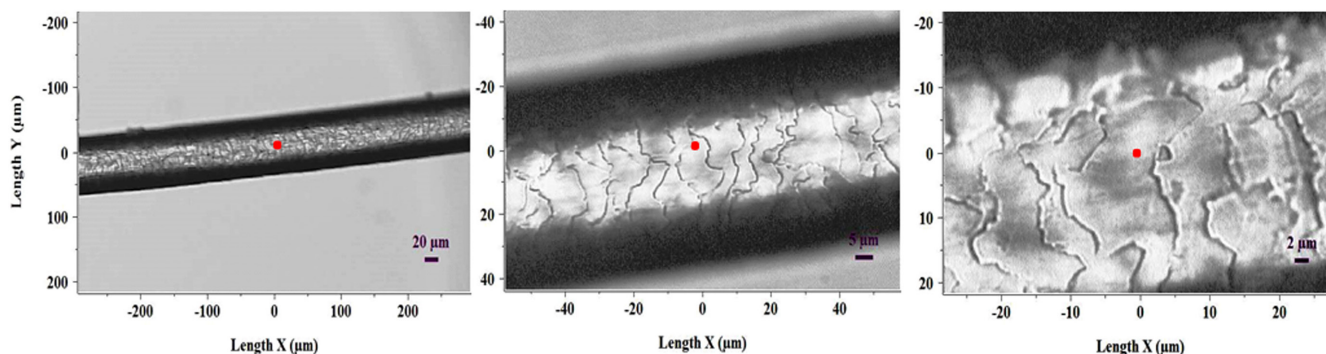
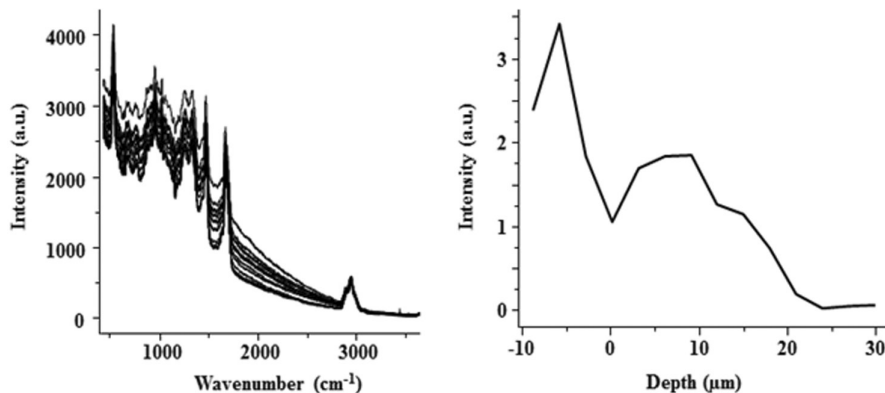


FIGURE 1 Light microscopy image of a hair fibre (10 $\times$ , 50 $\times$  and 100 $\times$ ) with the position of mapping ( $Z$ ) profile (central dot position) [Colour figure can be viewed at [wileyonlinelibrary.com](http://wileyonlinelibrary.com)]

**FIGURE 2** Raman mapping ( $Z$ ) profile showing the depth scanning through the hair fibre from the surface  $Z = 0$ – $30\ \mu\text{m}$  of depth



analysis was used to extract unresolved  $\alpha$ -helix and  $\beta$ -sheet keratin conformations from the hair fibres' spectra in the Amide I spectral band. This procedure was based on the least-squares method using Gaussian and Lorentzian functions. After the curve fitting, we have integrated  $\alpha$ -helix and  $\beta$ -sheets keratin marker, respectively, at ( $1640$ – $1660\ \text{cm}^{-1}$ ) and ( $1660$ – $1685\ \text{cm}^{-1}$ ) spectral regions. For S-S cysteine keratin cross-links bands, we have integrated the peak at  $510\ \text{cm}^{-1}$  [10].

## In-vivo tests

Two studies were conducted in accordance with the International Council for Harmonization (ICH), the Guidelines for Good Clinical Practice and the Declaration of Helsinki. All participants provided written informed consent prior to study beginning.

Both in use tests, of a 1-month duration, were performed on either 23 Caucasian subjects or 23 Asian subjects. They used the heat protective hair treatment on hair lengths and ends, under the normal condition of use, 3 times a week before using their own straightening iron or hair dryer.

Among the Caucasian subjects using a straightening iron, 5 of them with natural blond or light brown hair (in order to limit fluorescence interference during Raman measurements) were selected for the Raman spectroscopy analysis. A sampling of their hair (about 15–20 hair and 5–6 cm of length) was collected for analysis before hair treatment and after 1 month of use (with the last application 2 days before). The subjects answered a satisfaction questionnaire about hair care effect after 1 month of use, the percentage was calculated taking into account the positive answers.

An evaluation by a hairdresser, on the whole hair, was performed on the Caucasian panel based on a sensory analysis of 4 descriptors (brittle aspect, split aspect, repaired aspect of the hair and hair shininess) before and after 1 month. This evaluation was carried out using

structured scales defined by the references “no intensity” (limit 0) and “maximum intensity” (limit 10). The hairdresser evaluates the intensity of each descriptor by attributed a mark on the scale displayed on a computer screen on a specific software developed.

The improvement percentage was calculated and validated by statistical analysis. The results of both the satisfaction questionnaire and hairdresser assessment could be a support to claim that the product can beautify the hair despite having been heated.

## Statistical analysis

The results that followed a parametric distribution were subjected to statistical analysis using Student's  $t$ -test, while those that did not follow a parametric distribution were subjected to statistical analysis using the Mann–Whitney test.  $p$  values from significance scores are presented in figures as follows: \* $p$  value  $<0.05$ ; \*\* $p$  value  $<0.01$ ; \*\*\* $p$  value  $<0.001$ .

## RESULTS

### Preparatory study

In order to determine a heat stress threshold suitable for our study without causing significant damage on the hair fibre, different heat stress cycles (0, 5 and 10) were applied to hair fibres followed by morphological analysis by conventional microscopy on cross sections and by SEM on intact fibres. The heat stress cycles were applied using a hair iron straightener at  $235^\circ\text{C}$ .

Compared to untreated hair fibre, the results (Figure 3) of the conventional microscopy and the SEM show a significant degradation of the fibre structure at 10 stress cycles by the formation of bubbles and cracks.

These results show that 10 heat stress cycles are too aggressive on the hair structure and cause significant

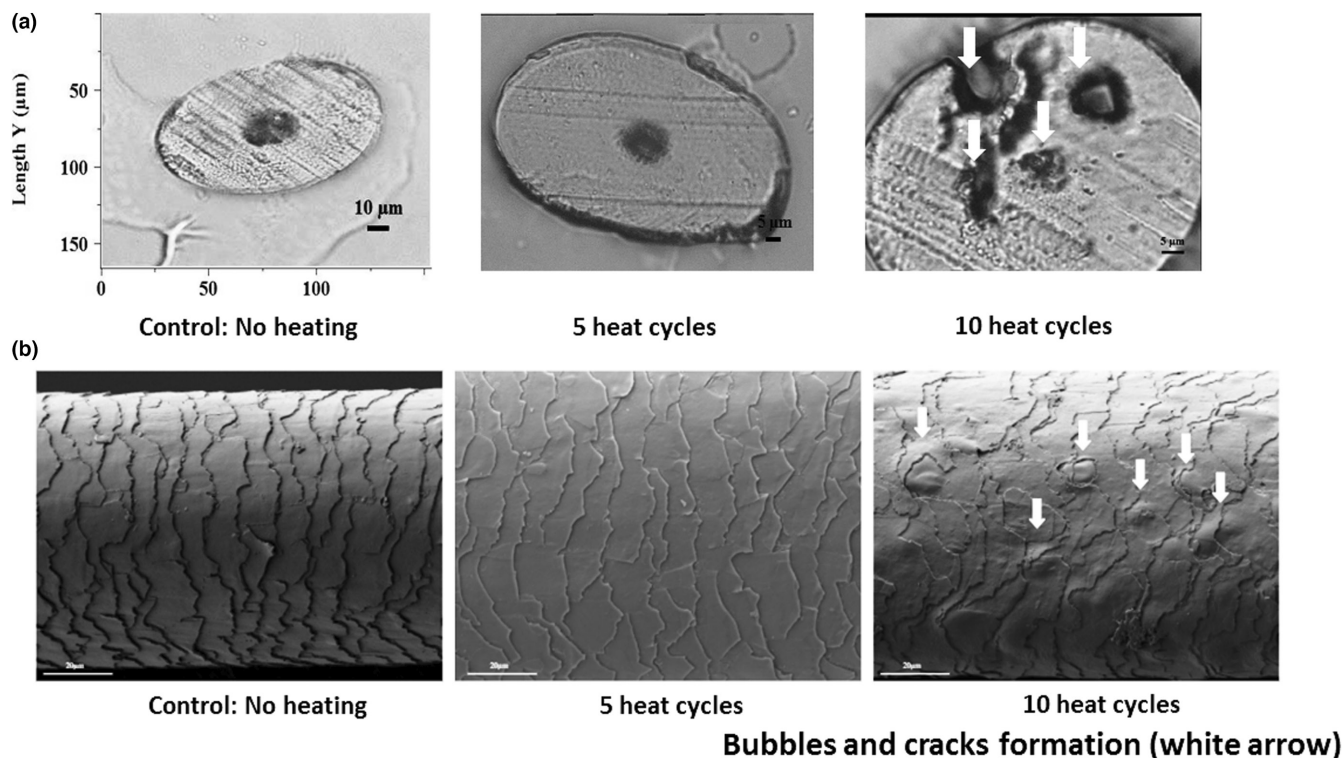


FIGURE 3 Light microscopy images (100 $\times$ ) of cross section of hair fibres subjected to (0, 5 and 10) heat stress cycles (a) and SEM images ( $\times 10000$ ) of hair fibres subjected to (0, 5 and 10) heat stress cycles (b) (formation bubbles and cracks indicated by white arrows)

morphological alteration of the fibres by the appearance of bubbles and cracks. Based on these results, we chose to conduct our study with two different heat stress thresholds. For the SEM technique, a 10 heat cycle threshold was chosen because this threshold allows observing morphological modifications on the hair structure fibre. For the CRS technique, a lower heat stress threshold at 5 cycles was chosen to preserve the morphological integrity of the hair fibres in order to focus the study on molecular changes after heat stress.

### Evaluation of thermal stress on the hair by SEM method

This technique was used to evaluate the effect of exposing the surface of the hair fibre to excess heat (235°C). Figure 4 shows the SEM images of hair fibres that were subjected to 10 cycles of thermal treatment using a hair iron straightener at 235°C. The SEM pictures below are representative of the obtained effect of heat on untreated and treated hair with the hair care product.

The pictures show substantial damage of heat on untreated hair fibres by the appearance of bubbles and cracks. These phenomena were as expected: the inner part of hair contains about 10% of “bound water” (water bound to keratin chains). This water contained in hair fibres

gives the hair its elasticity and suppleness. Heat stress induces the “boiling” of this water and tiny vapour bubbles (also called heat bubbles) are formed inside the hair fibres. These water vapour bubbles deform the hair from the inside by exerting pressure on the constituent parts of the fibre and hair loses its flexibility and becomes very brittle [3]. Heating devices induce crackles on hair fibres by altering the natural lipidic film that protects the hair fibre surface.

The tested hair care product clearly shows protective properties with respect to heat damage. Hair treatment with the test product before heat damage systematically showed lesser “bubbles” and “crackling” on the hair surface.

### Evaluation of thermal stress on the hair by Raman spectroscopy

#### Assignments of keratin markers in Raman spectra of human hair fibre

The first step of this work was to determine the reference Raman spectra of all hair samples and to compare them with reference human keratin Raman signal. The corresponding Raman spectrum is shown in Figure 5. The comparison between Raman spectra of human hair fibres and

**FIGURE 4** SEM image of hair fibres after 10 cycles of thermal stress ( $\times 500$  a and b), ( $\times 1000$  c and d) with and without treatment with the hair care product (formation of bubbles and cracks indicated by white arrows)

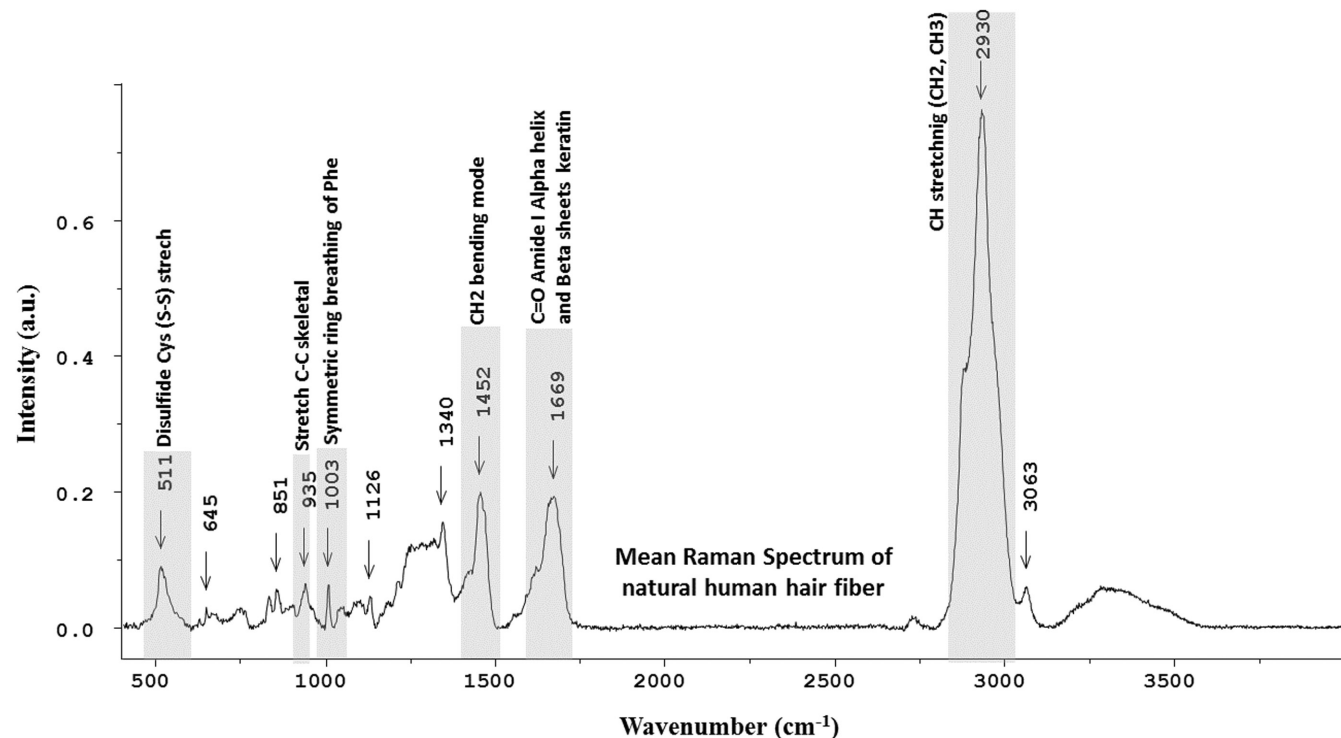
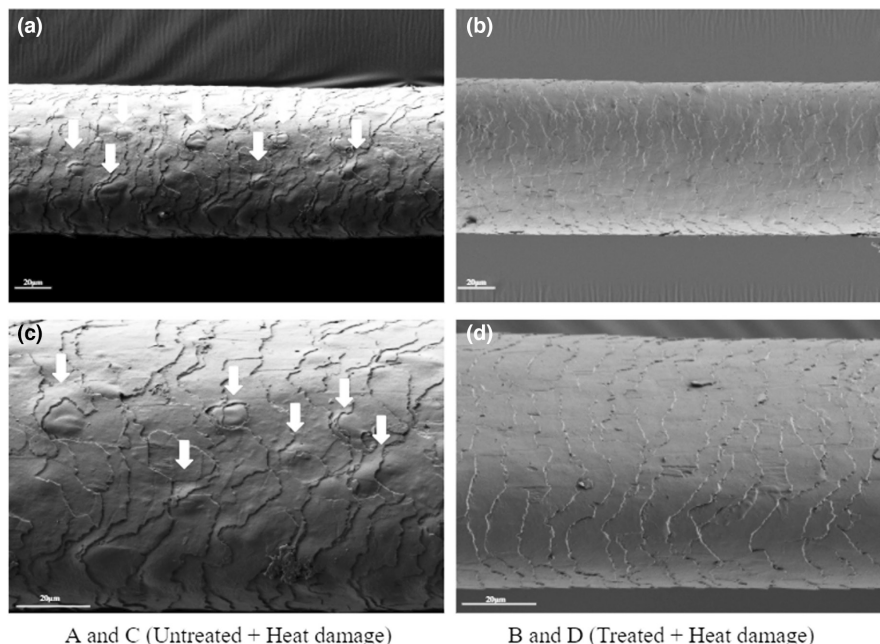


**FIGURE 5** Raman spectrum of human hair fibre showing keratin molecular markers (highlighted) after thermal stress

pure keratin molecules allowed us to evaluate the contribution of the keratin molecule to the hair fibre spectrum and the assignment of specific keratin bands in the global spectrum of human hair. The results show very close spectral signatures between hair samples and reference keratin Raman signal. In the spectra, several peaks specific to keratin molecules can be distinguished (highlighted bands in Figure 5) and the major bands are found in two spectral windows:  $400\text{--}1700\text{ cm}^{-1}$  and  $2700\text{--}3000\text{ cm}^{-1}$  [10].

### Raman ex-vivo analysis

To investigate the influence of treatments with hair product and thermal stress with straightening process on hair fibres; the keratin structure of 4 samples [S1: untreated and unheated (Control), S2: treated and unheated (T UH), S3: untreated and heated ( $5\times$ ) (UT H) and S4: treated and heated ( $5\times$ ) hair sample (T H)] of natural human hair was directly analysed by using confocal Raman spectroscopy.



We recorded 3 Raman ( $Z$ ) profiles directly on the human hair fibre resulting from each treatment. Before the data analysis, the Raman signal of the product has been checked and does not show any interference with the hair keratin signal in the spectral region of interest (Amide I and S-S disulfide bands). The spectral comparison of the hair samples with the product is shown in [Figure 6](#).

To estimate the spectral difference, the mean Raman spectra of the 4 hair samples were compared and the corresponding spectra were classified by using a hierarchical cluster analysis algorithm. The function used calculates Euclidean distances between the spectra and the group according to their similarities in a cluster. The results are shown in [Figure 7](#).

The results of this spectral classification based on the mean spectra, allowed to distinguish four spectral groups corresponding, respectively, to the S1, S2 S3 and S4 samples. These results show that the Raman spectral signature of the treated and heated hair fibre (S4 sample) is very close to the negative control (untreated and unheated S1 sample) (framed samples) compared to the S2 and S3 samples. The S3 hair sample (untreated and heated) shows the maximum spectral heterogeneity threshold (5) compared to the other hair samples (S1, S2 and S4). This classification suggests that the keratin spectral signature is preserved by hair product after thermal stress with the straightening process.

To investigate which molecular component of keratin the product has a significant effect, the Raman spectra of the 4 hair samples are submitted to a statistical analysis to determine whether there are significant differences between them. The comparison between mean spectra of negative control (S1) and the means spectra of each hair sample (S2, S3 or S4) by using the Mann–Whitney statistical test ( $p = 0.05$ ) allowed possible to determine the most pertinent spectral markers for detecting the molecular changes in the keratin. The spectral comparisons show a specific and non-specific spectral variability, the amide I and disulfide S-S cysteine keratin bands are identified as a discriminant between the samples after hair treatment with the product and after thermal stress; these results suggest that the hair product has a molecular effect on these molecular bands. For this, the spectral analysis was particularly focused on the amide I and disulfide S-S cysteine bands. The more keratin hair fibres are constructed almost exclusively of  $\alpha$ -helices and are rich in cysteine which provides covalent disulfide (S-S at  $510\text{ cm}^{-1}$ ) cross-links between adjacent polypeptide chains.

The amide I region allows detecting the change in  $\alpha$ -helix and  $\beta$ -sheet keratin conformation. To evaluate the influence of treatment and thermal stress on hair fibres two molecular spectral markers were calculated: the ratio

of  $\alpha$ -helix ( $1640\text{--}1660\text{ cm}^{-1}$ ) to  $\beta$ -sheets ( $1660\text{--}1685\text{ cm}^{-1}$ ) on amide I region and disulfide S-S cysteine keratin cross-links bands ( $510\text{ cm}^{-1}$ ).

The results are shown in [Figure 8](#). These results show that the thermal stress has a tendency to decrease the  $\alpha$ -helix keratin conformation (for S3 and S4 samples) ([Figure 8](#), graph a). In parallel, significant increase in  $\beta$ -sheets keratin conformation is observed for S3 sample (untreated and heated) ([Figure 8](#), graph b), and this increase is not significant for treated hair samples (S2 and S4). These variations in  $\alpha$ -helix and  $\beta$ -sheets keratin conformation cause a significant decrease in the ratio of  $\alpha$ -helix to  $\beta$ -helix sheets keratin band for S3 sample (untreated and heated) ([Figure 8](#), graph c). This result can be explained by the fact that the product provides thermal protection of the hair fibres by promoting the  $\alpha$ -helix keratin conformation and inhibits the transition to the  $\beta$ -sheets keratin conformation.

Disulfide bonds are important for the stabilization of folding structure of keratin. The stability of S-S disulfide bonds in keratin can be assessed by calculating the conformational order of disulfide S-S cysteine bonds in the  $474\text{--}578\text{ cm}^{-1}$  spectral range. The results are shown in graph ([Figure 9](#)).

These results show that the thermal stress decreases the intensity of covalent cross-links bands of cysteine for S3 sample (untreated and heated). This can be explained by a fragility in the keratin structure caused by thermal stress. In parallel, for S4 sample (treated and heated), we observe stability in the S-S disulfide keratin bands, suggesting that the product preserves the (S-S) disulfide keratin bands from thermal damage and stabilize the tertiary structure of keratin hair fibre.

## Raman in-vivo analysis

In order to confirm the results obtained from ex vivo analysis, a complementary in vivo study was carried out on volunteers. For this, 5 volunteers with light blond hair were included in this analysis and two hair samples per subject were taken. The first hair sample on D0 before product application and the second hair sample at 28 days (D28) after product applications and thermal stress. As for ex vivo analysis, the molecular analysis was particularly focused on the disulfide S-S and amide I keratin bands. The results are shown in graphs ([Figure 10](#)). As observed for ex vivo analysis, the ratio of  $\alpha$ -helix to  $\beta$ - sheets keratin conformation increases significantly at D28 after hair treatment and a tendency (limit to significance) to decrease in the S-S disulfide keratin bands was observed. These results confirm our

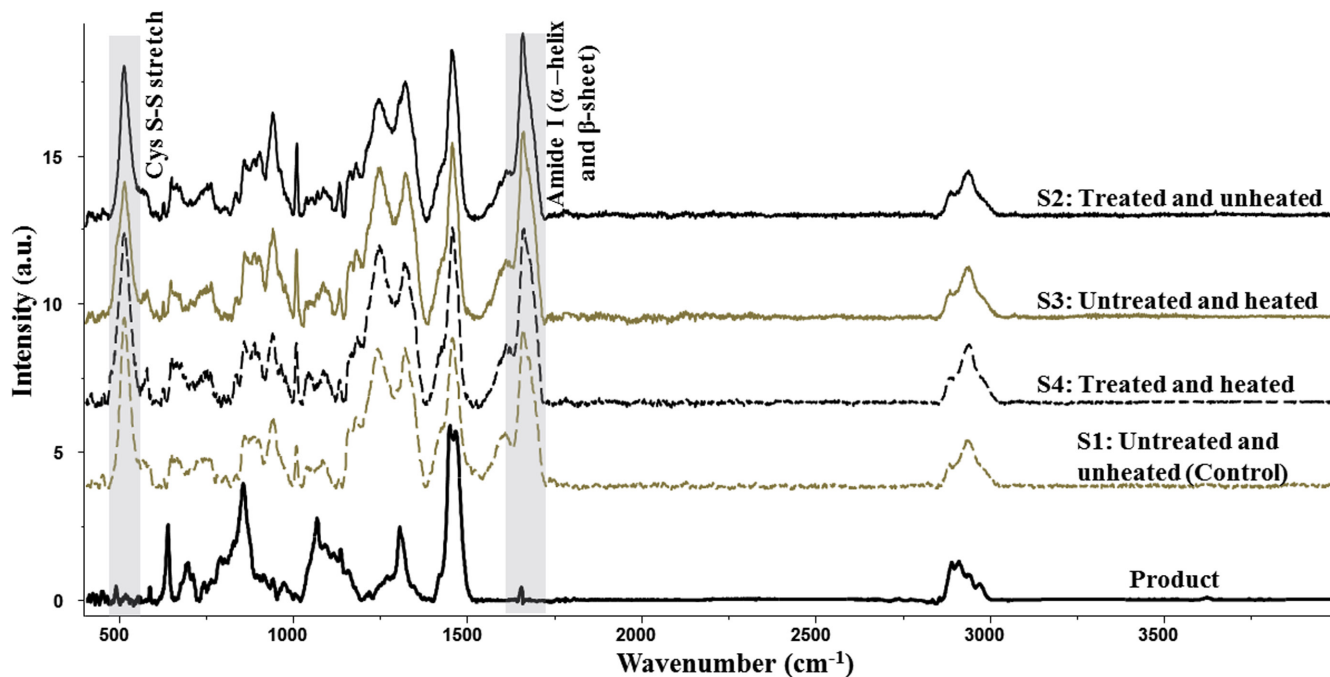
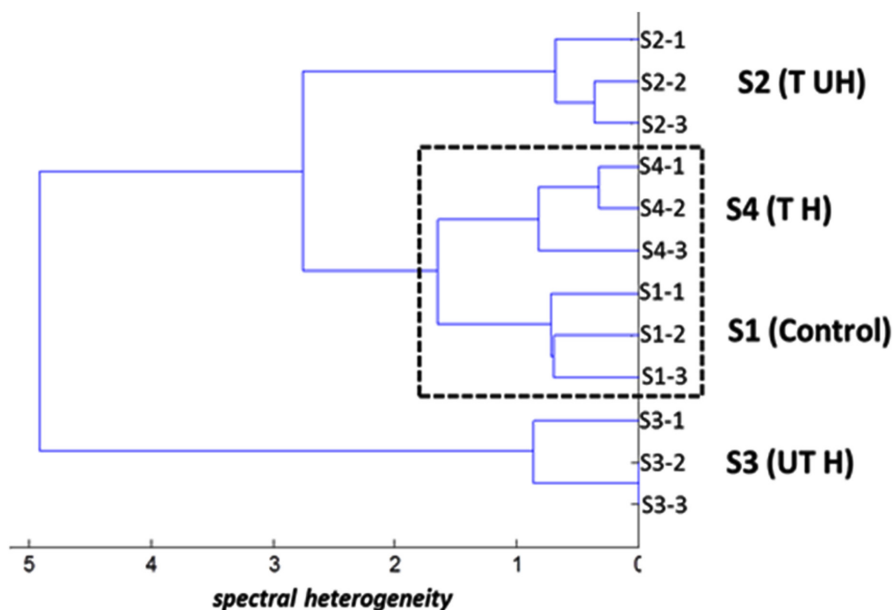


**FIGURE 6** Spectral comparison between hairs samples spectra (S1, S2, S3 and S4) and tested product spectrum. The highlighted peaks represent the spectral regions of interest [Colour figure can be viewed at [wileyonlinelibrary.com](http://wileyonlinelibrary.com)]

**FIGURE 7** Hierarchical cluster analysis of mean Raman spectra of 4 hair samples. S1: untreated and unheated (Control), S2: treated and unheated (T UH), S3: untreated and heated (5×) (UT H) and S4: treated and heated (5×) (T H) [Colour figure can be viewed at [wileyonlinelibrary.com](http://wileyonlinelibrary.com)]



hypothesis, suggesting that the hair product promotes the  $\alpha$ -helix keratin conformation and contributes to the stability of its tertiary structure.

### Evaluation of the hair care effect during the clinical study

Furthermore, these results were also completed with another analysis and enable to validate the efficiency of the hair care from a consumer and a hairdresser point of view.

The hairdresser assessed an immediate decrease of 37% of the brittle aspect of the hair and of 30% of split hair as well as an increase, after 1 month of use, of 17% of the hair shininess and of 26% of a repaired hair aspect. After 1 month of use, the satisfaction questionnaire revealed the following results (Figure 11).

### DISCUSSION

In this study, the evaluation of a thermal protection of a cosmetic finished product with several methods provided

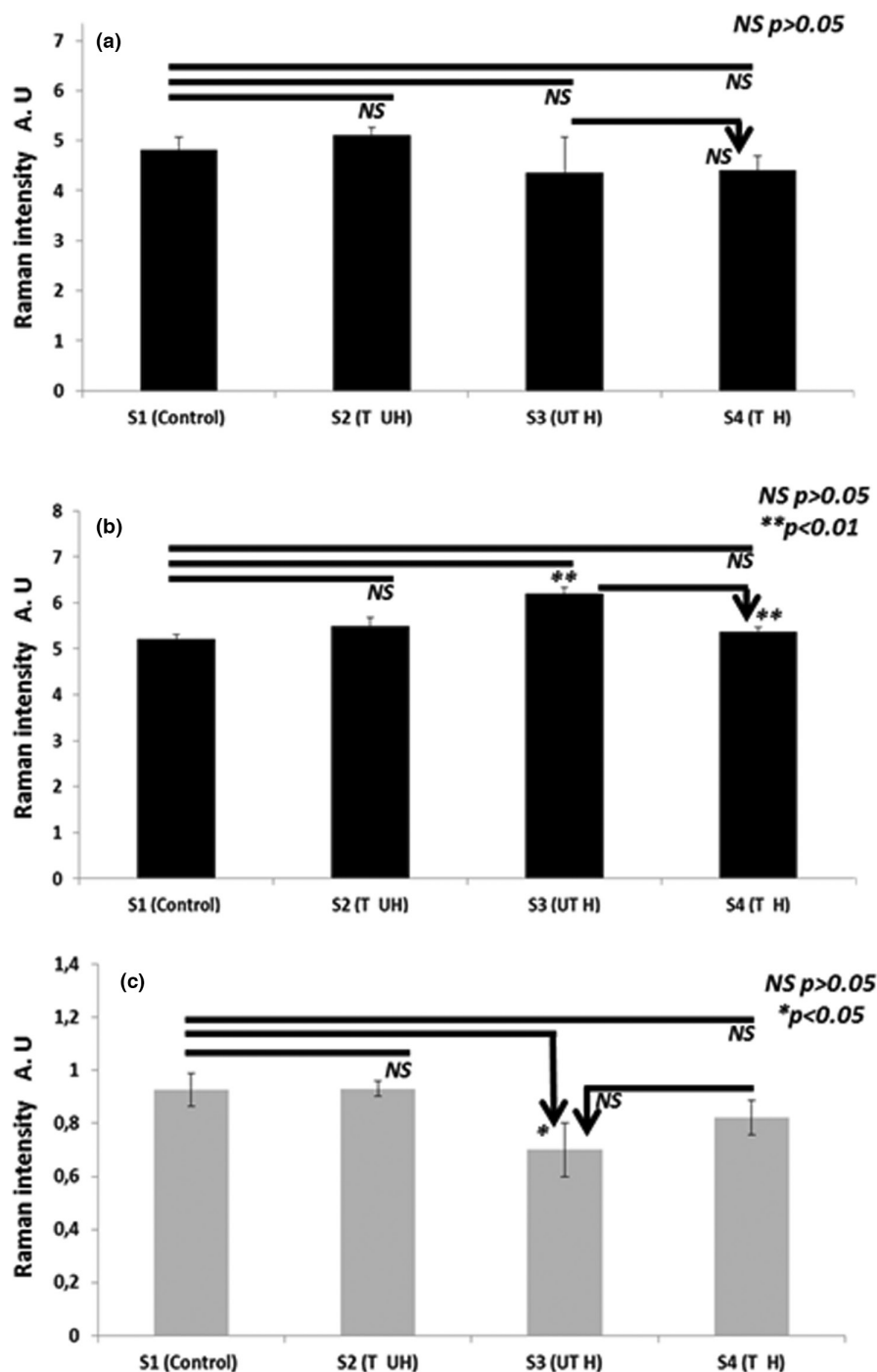


FIGURE 8 Evolution of  $\alpha$ -helix (a),  $\beta$ -sheets (b) and ratio  $\alpha$ -helix/ $\beta$ -sheets (c) keratin conformation of 4 hair samples. Data are shown as the mean  $\pm$  standard error (\*\* $p < 0.01$ , \* $p < 0.05$ , NS: not significant  $p > 0.05$ ). S1: untreated and unheated (Control), S2: treated and unheated (T UH), S3: untreated and heated (5 $\times$ ) (UT H) and S4: treated and heated (5 $\times$ ) (T H)

interesting information on the effect of the thermal stress on hair fibres. This hair care product acts through thermoactive technology formed by two ionic polymers. Activated by heat, this product forms an adhesive microgel that helps the appearance of hair by closing scales and filling in breaks. Thus, the fibre should be protected from the heat, the hair is shinier, softer and more supple with less split ends and less brittle hair.

The SEM method enabled the evaluation of the effect of excess heat on hair fibres. The obtained images showed changes in the hair surface after a thermal stress. Two main deformation patterns were observed: cracks on

hair cuticles and bubble formation in the hair fibres. The treatment of the hair fibres with the hair care product decreased the heat associated damage.

At the molecular level, the results of Raman spectroscopy showed, on the one hand, that the product provides thermal protection of the hair fibres by promoting the  $\alpha$ -helix keratin conformation and inhibits the transition to the  $\beta$ -sheets keratin conformation. On the other hand, for treated and heated hair samples, we observed stability in the S-S disulfide keratin bands and this suggests that the product preserves the (S-S) disulfide keratin bands from thermal damage.

According to our results, we can suppose that the product provides thermal protection of the hair fibres by acting at two levels of keratin molecular structure: (i) at secondary structure by promoting the  $\alpha$ -helix keratin conformation and (ii) at tertiary structure by protecting hydrogen keratin bonds and stabilization of disulfide bridges. These results are consistent with the thermal protective claims of the product and with the morphological observations made in SEM.

However, we have confirmed the Raman and SEM results with other techniques, such as the repairing effect on the split ends of the hair fibres, the evaluation of the protection of hair's lipid envelope by fluorescence microscopy on hair fibres cross-sections and Differential Scanning Calorimetry (DSC) (Supplementary Data: S1).

Furthermore, these results were also confirmed by the Asian and Caucasian consumers and a hairdresser. After 1 month of use, most of the consumers found that their hair was protected from the heat of styling

appliances by protecting hair against split ends and brittle hair. The hair was shinier, softer, more supple and thus more beautiful; those improvements were also found by the hairdresser. However, these results need to be confirmed on more donors by combining other factors affecting heat-protecting effect of product such as (origin, colour, age and sex ...).

## CONCLUSIONS

Through the results obtained in this work, we have demonstrated by the Raman spectroscopy technique that the hair care product has thermal protective activity by acting on the conformation and disulfide bridges of keratin. However, by SEM analysis, we established a link between the molecular action of the product and the preservation of hair fibre morphology against thermal damage, such as

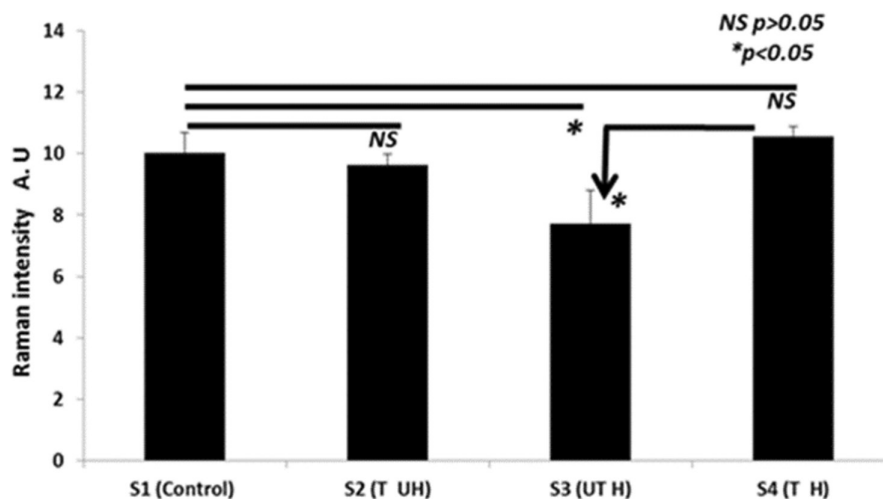


**FIGURE 9** Evolution of disulfide (S-S) cross-links band of 4 hair samples. Data are shown as the mean  $\pm$  standard error of the disulfide (S-S) cross-links band (\*\* $p < 0.01$ , \* $p < 0.05$ , NS: not significant  $p > 0.05$ ). S1: untreated and unheated (Control), S2: treated and unheated (T UH), S3: untreated and heated (5 $\times$ ) (UT H) and S4: treated and heated (5 $\times$ ) (T H)

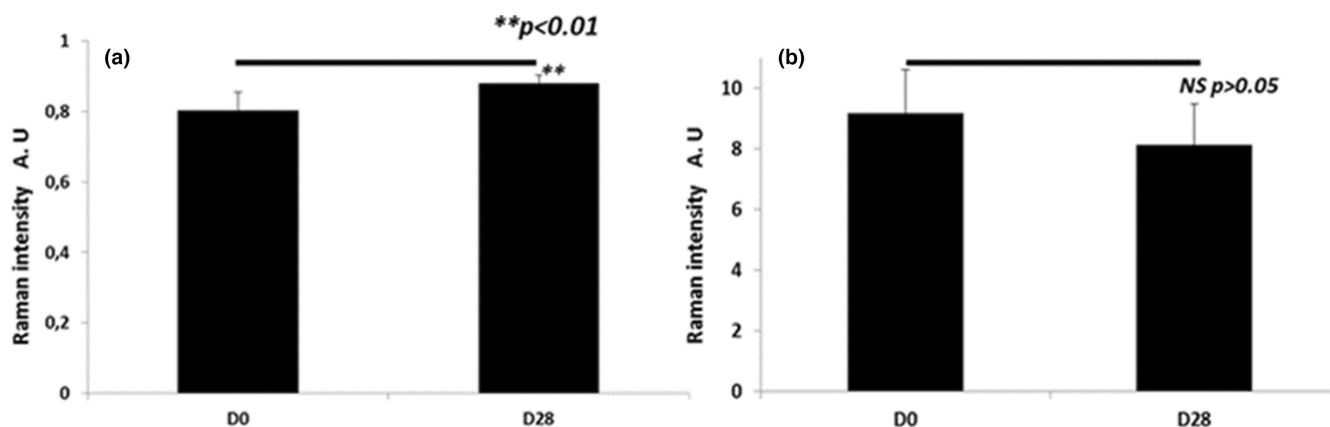


**FIGURE 10** Evolution of  $\alpha$ -helix/ $\beta$ -sheets keratin conformation (a) and disulfide (S-S) cross-links band (b) of in-vivo hair samples (\*\* $p < 0.01$ , \* $p < 0.05$ , NS: not significant  $p > 0.05$ ). D0 before product application, D28 after product application and thermal stress

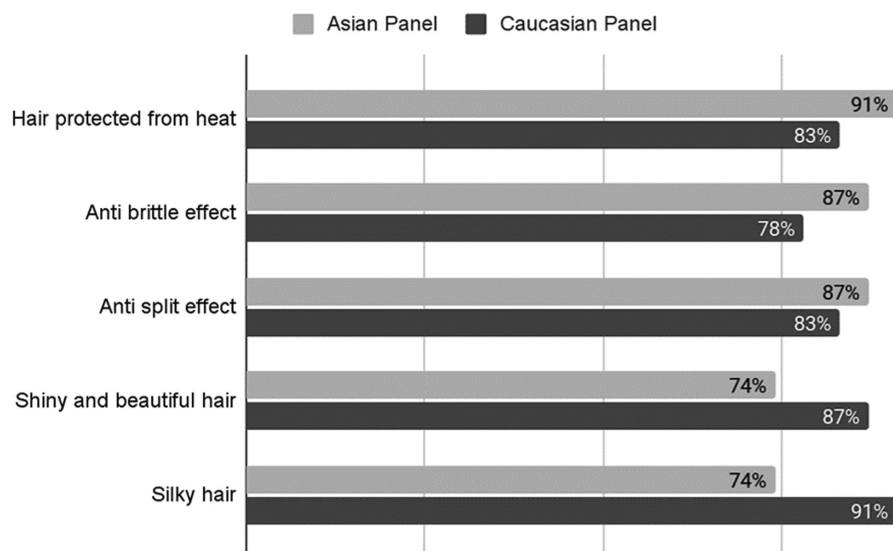


FIGURE 11 Satisfaction results of the in use tests on the Asian and on the Caucasian panels. Percentage of positive answers

bubbles and cracks. Moreover, a complementary clinical study confirms the results obtained with the SEM and the Raman spectroscopy by showing a good perception by the subjects of the thermo-protective effect provided by the hair care treatment as well as the overall beautifying effect on the hair.

According to our results, Raman spectroscopy is a technique with a great molecular potential that offers the opportunity to evaluate other important aspects related to the effectiveness of cosmetics on human hair such as hydration, active penetration, oxidative and UV stress and this without performing any labeling or sample extraction.


### ACKNOWLEDGEMENTS

The authors would like to thank the PICT platform (Plateforme d'Imagerie Cellulaire et Tissulaire) of the University of Reims Champagne-Ardenne (France) for the technical support in Confocal Raman Spectroscopy.

### CONFLICT OF INTEREST

None.

### ORCID

Mohammed Essendoubi  <https://orcid.org/0000-0002-0136-0767>

### REFERENCES

- Bloch LD, Goshiyama AM, Dario MF, Escudeiro CC, Sarruf FD, Velasco MVR, et al. Chemical and physical treatments damage Caucasian and Afro-ethnic hair fiber: analytical and image assays. *J Eur Acad Dermatol Venereol*. 2019;33:2158–67.
- Gamez-Garcia M. The cracking of human hair cuticles by cyclical thermal stresses. *J Cosmet Sci*. 1998;49:141–53.
- Gamez-Garcia M. Void and pore formation inside the hair cortex by a denaturation and super-contraction process occurring during hair setting with hot irons. *J Cosmet Sci*. 2011;62:109–20.
- Rudnicka L, Olszewska M, Waśkiel A, Rakowska A. Trichoscopy in hair shaft disorders. *Dermatol Clin*. 2018;36:421–30.
- Stanić V, Bettini J, Montoro FE, Stein A, Evans-Lutterodt K. Local structure of human hair spatially resolved by sub-micron X-ray beam. *Sci Rep*. 2015;30:5:17347.
- Fukuda M, Marubashi Y, Nawa T, Ikuyama R. Structural analysis of macrofibrils in a human permanent waved hair by scanning microbeam small-angle X-ray scattering measurements. *J Cosmet Sci*. 2018;69:121–30.
- Fedorkova MV, Brandt NN, Chikishev AY, Smolina NV, Balabushevich NG, Gusev SA, et al. Photoinduced formation of thiols in human hair. *J Photochem Photobiol*. 2016;164:43–8.
- Kadir M, Wang X, Zhu B, Liu J, Har-land D, Popes Cu C. The structure of the “amorphous” matrix of keratins. *J Struct Biol*. 2017;198:116–23.
- Turner EA, Stenson AC, Yazdani SK. HPLC-MS/MS method for quantification of paclitaxel from keratin containing samples. *J Pharm Biomed Anal*. 2017;139:247–51.
- Essendoubi M, Meunier M, Scandolera A, Gobinet C, Manfait M, Lambert C, et al. Conformation changes in human hair keratin observed using confocal Raman spectroscopy after active ingredient application. *J Cosmet Sci*. 2019;41:203–12.
- Sandt C, Borondics F. A new typology of human hair medullas based on lipid composition analysis by synchrotron FTIR microspectroscopy. *Analyst*. 2021;146:3942–54.
- Kim KS, Shin MK, Park HK. Effects of scalp dermatitis on chemical property of hair keratin. *Spectrochim Acta A Mol Biomol Spectrosc*. 2013;109:226–31.
- Lau K, Hedegaard MA, Kloepper JE, Paus R, Wood BR, Deckert V. Visualization and characterisation of defined hair follicle compartments by Fourier transform infrared (FTIR) imaging without labelling. *J Dermatol Sci*. 2011;63:191–8.
- Lam SE, Mat Nawi SN, Abdul Sani SF, Khandaker MU, Bradley DA. Raman and photoluminescence spectroscopy analysis of gamma irradiated human hair. *Sci Rep*. 2021;11(1):7939.

15. Pienpinijtham P, Thammacharoen C, Naranitad S, Ekgasit S. Analysis of cosmetic residues on a single human hair by ATR FT-IR microspectroscopy. *Spectrochim Acta A Mol Biomol Spectrosc.* 2018;197:230–6.
16. Zhang G, Senak L, Moore DJ. Measuring changes in chemistry, composition, and molecular structure within hair fibers by infrared and Raman spectroscopic imaging. *J Biomed Opt.* 2011;16:056009.

### SUPPORTING INFORMATION

Additional supporting information can be found online in the Supporting Information section at the end of this article.

**How to cite this article:** Essendoubi M, Andre N, Granger B, Clave C, Manfait M & Thuillier I et al. New approach for hair keratin characterization: Use of the confocal Raman spectroscopy to assess the effect of thermal stress on human hair fibre. *Int J Cosmet Sci.* 2022;44:588–601. <https://doi.org/10.1111/ics.12808>